

another structure, the situation may be reversed. It is therefore useful to have available a variety of methods incorporating as many different approaches as possible. The *SYSTEM90* approach is quite distinctive and we have shown that it stands comparison with other existing methods in its effectiveness.

Anyone wishing to obtain *SYSTEM90*, together with full information on its use, can do so by applying to HY.

The authors are grateful to Professor M. M. Woolfson for his interest in this project and his encouragement. The *SYSTEM90* program system was tested by Professor Fan Hai-fu and Professor Gu Yuan-xin, who provided data and were most helpful. HY also expresses his gratitude to his

advisor Professor Tang You-qi and to Professor Fu Heng and the Director and other senior scientists in the Institute of Chemistry. All of the above helped in the success of this project, which was supported by the NSFC, the Academia Sinica and the Laboratory for Structural Chemistry of Unstable and Stable Species. The authors also thank the referees for advice on the better presentation of this work.

References

- BHAT, T. N. (1990). *Acta Cryst.* **C46**, 112–116.
 DEBAERDEMAEKER, T., TATE, C. & WOOLFSON, M. M. (1988). *Acta Cryst.* **A44**, 353–357.
 FAN, H., YAO, J. & QIAN, J. (1990). *Acta Cryst.* **A46**, 99–103.
 HULL, S. E. & IRWIN, M. J. (1978). *Acta Cryst.* **A34**, 863–870.
 KARLE, J. & HAUPTMAN, H. (1956). *Acta Cryst.* **9**, 635–651.

Acta Cryst. (1994). **A50**, 753–759

The Density of Three-Dimensional Nets

BY S. T. HYDE

Applied Mathematics Department, Research School of Physical Sciences, Australian National University, Canberra 0200, Australia

(Received 3 January 1994; accepted 10 May 1994)

Abstract

Estimates for the density of periodic three-dimensional nets in Euclidean three-dimensional space (\mathbb{R}^3) are derived. The analysis assumes that the nets tile triply periodic hyperbolic surfaces that are free of self-intersections (embedded in \mathbb{R}^3). Upper and lower bounds of the net density as a function of the average ring size on the surfaces are given. These geometrical relations are compared with framework densities of a range of silicon-rich zeolites, silica clathrasils and dense four-connected silicates in order to separate the roles of geometry and chemistry in setting silicate densities. The data suggest that silica frameworks are constrained by an approximate requirement of constant area per framework vertex in addition to the impositions of Euclidean three-space and are thus hyperbolic two-dimensional (layer) structures.

Introduction

Although nets have intrinsic mathematical interest (as 'graphs'), their geometrical characteristics are of relevance also to the solid state. In particular, the bonding topology of covalent frameworks – such as

silicates – can be represented by a three-dimensional network. This has led to a number of theoretical studies of three-dimensional nets and their possible realizations as chemical frameworks (Wells, 1977; Smith, 1988; O'Keeffe, 1991). Despite the universal use of nets to describe structures in the solid state (any chemistry text is replete with examples), little fundamental work has been done. O'Keeffe has conjectured a number of challenging results and conjectures about three-dimensional nets, which suggest that the variety of three-dimensional nets realizable in Euclidean three-dimensional space is more limited than intuition would suggest. As yet, no procedure has been found for a systematic enumeration of three-dimensional networks (hereafter referred to as 'nets'), so it is difficult to establish their general characteristics.

Some intriguing relations between the bulk density of periodic nets and their topology have been reported. The relation between silicate densities and ring sizes has been reported and analysed to a limited extent by Stixrude & Bukowinski (1990). Nets of low density (number of vertices per unit volume), called 'rare' nets, are of interest as possible structure for zeolites. In this context, approximate relations between the net density and the size of the smallest

rings in the net have been noticed: in general, rare nets have a significant proportion of small rings (Meier, 1986; Brunner & Meier, 1989; O'Keeffe, 1991). Conversely, O'Keeffe's results suggest that dense nets contain large rings. (A 'ring' in the net is a closed path confined to edges of the net.) A theoretical explanation of these trends remains elusive. An analytical result for the net density has recently been derived, under the twin assumptions that the net edges lie in a triply periodic hyperbolic surface (which is approximated by a triply periodic minimal surface) and that the area per net vertex on the surface (the hyperbolic surface density) is fixed for a single stoichiometry (e.g. SiO₂), regardless of the net and surface topology (Hyde, Blum & Ninham, 1993; Hyde, 1993). This result is consistent with a qualitative trend of increasing net density with ring size.

In this note, I adopt the two-dimensional hyperbolic approach. The analysis is not confined to chemical frameworks; rather, I am concerned with the geometrical characteristics of a small selection of three-, four-, five- and six-connected nets. I focus on the net density and derive bounds for densities of nets as a function of the average ring size of the net rings that lie in the surface.

Nets and hyperbolic surfaces

König's theorem ensures that any connected network can be embedded in an orientable surface (Lindsay, 1959). Three-dimensional nets can be embedded in (orientable) hyperbolic surfaces, just as planar nets can be viewed as tilings of the plane (Hyde & Andersson, 1984).

Nets that describe the edges of 'infinite' (Wells, 1977) or 'skew' (Coxeter, 1937) polyhedra tessellate hyperbolic surfaces that are free of self-intersections and dissect space into two intertwined labyrinths. These nets are generally of low density, such as many (four-connected) nets describing zeolite frameworks. For example, the nets describing the analcime and sodalite frameworks (Meier & Olson, 1992) can be drawn on the *D* and gyroid triply periodic minimal surfaces (Andersson, Hyde, Larsson & Lidin, 1988). In other cases, the nets lie in hyperbolic surfaces that are not strictly minimal surfaces, but rather parallel surfaces or surfaces of constant (nonzero) mean curvature related to minimal surfaces.

Dense nets can be placed onto surfaces containing self-intersections. However, a number of these examples can also be placed onto intersection-free surfaces. For example, edges of the NbO (Wells, 1977) and CdSO₄ (O'Keeffe & Hyde, 1994) nets are straight lines on the *D*-surface and its tetragonal relative, the *tD*-surface, respectively. It is not known whether all nets can be placed on intersection-free surfaces.

It is important to recognize that a single net can be embedded in a variety of (orientable) surfaces. For example, complementary periodic minimal surfaces contain the same set of straight lines (Hyde & Anderson, 1984), thus a net containing any subset of those lines can be embedded in either surface. The surfaces that can be reticulated by the net are topologically distinguishable, *i.e.* they have a different Euler characteristic, χ , per unit cell. (For orientable surfaces, χ is given by the expression $\chi = 2 - 2g$. Here g is the genus of the surface per unit cell, which is equal to the number of holes in a unit cell of the surface that are not related by lattice translation vectors.) Topologists refer to a 'minimal' embedding, which sets the 'characteristic', γ , of the net (Firby & Gardiner, 1991). The value of γ is equal to the *maximum* χ (*i.e.* the minimum genus per unit cell) among all surfaces that can be tessellated by the net. (The corresponding surface is termed the 'minimal surface' for the graph, not to be confused with the differential geometric sense of 'minimal surfaces' – surfaces of zero mean curvature – used exclusively in this paper.)

Once nets are realized as tessellations of hyperbolic surfaces, the net density can be readily related to the density of vertices on the surface and the curvatures of that surface. The surface density is related to the surface area of the surface and the area per net vertex. The link between the area per unit cell of a periodic hyperbolic surface, *S*, the Euler characteristic of the surface per unit cell, χ , and the unit-cell volume, *V*, can be neatly characterized by the dimensionless variable, which I call the 'homogeneity index', *H*:

$$H \equiv S^{3/2}(-2\pi\chi)^{-1/2}V^{-1}. \quad (1)$$

The density of the net is the number of vertices per unit volume. In this note, I consider solely nets of equal edge length, *l*. The net 'rarity' *r* (O'Keeffe, 1991) is defined by the relation $r \equiv Nl^3/V$, where *N* is the number of net vertices per unit cell. If the scaled (curved surface) area per vertex in a given embedding surface is denoted Ω (= area per vertex/*l*²), (1) can be rewritten

$$H = [\Omega^{3/2}/(-2\pi\chi/N)^{1/2}]r$$

or

$$r = (H/\Omega^{3/2})(-2\pi\chi/N)^{1/2}. \quad (2)$$

The quantity $2\pi\chi/N$ is the integral (Gaussian) curvature per vertex. This is related to the average connectivity of the net, *z*, and the average ring size of all rings lying in the surface, *n*₂. Here, I take 'rings' to be shortest rings on the surface. All those rings that cannot be contracted continuously to a point – remaining at all stages on the surface – are excluded. Thus, for example, 'collar' rings, that surround tun-

nels of the intersection-free hyperbolic surfaces, do not contribute to n_2 (Hyde *et al.*, 1993).

Euler's relation between faces, edges and vertices on a (compactified) unit cell of the surface demands

$$\chi/N = \{z + [1 - (z/2)]n_2\}/n_2. \quad (3)$$

This yields the result

$$r/H = \Omega^{-3/2}[-2\pi(\{z + [1 - (z/2)]n_2\}/n_2)]^{1/2}. \quad (4)$$

This curved two-dimensional geometrical approach leads to a particularly simple expression relating the net density to the topological characteristics of the net, provided the magnitudes of H and Ω can be found.

For hypothetical 'homogeneous' hyperbolic surfaces, whose Gaussian curvature is everywhere constant and whose mean curvature is equal to zero, H is equal to $3/4$ (Hyde, 1992). The magnitude of the Gaussian curvature is dependent on the edge length, vertex angles and net torsion (Hyde *et al.*, 1993). Thus, nets whose vertex geometry is similar for all vertices ('quasi-uniform' nets) are expected to lie on quasi-homogeneous surfaces.

The value of Ω is less readily estimated. In the case of a number of silicate, water, silicon and germanium frameworks, the area has been found to be approximately constant within each chemical class, provided the surface has been chosen so that the value of n_2 is minimized (*i.e.* $\chi = \gamma$, so that the 'minimal embedding' is adopted) (Hyde, 1993). Equation (4) can be used to determine the universality of this finding. In this note, I consider nets in their *maximum-volume* form, realized when the nets adopt their most symmetric embedding (O'Keeffe, 1991). These embeddings are expected to approach most nearly the assumption of homogeneity discussed above.

The nets are listed in Table 1, along with associated geometric data. The estimation of H is done as follows. With the assumption that the embedding surfaces are parallel to minimal surfaces, the element of area of the embedding surface, S , is related to the corresponding area of the associated minimal surface, S_0 , and the Gaussian curvature of the minimal surface, K , by the equation

$$S = S_0(1 + Kx^2).$$

If the average radius of curvature for the minimal surface is R , $K = -R^{-2}$ so

$$S = S_0[1 - (x/R)^2]. \quad (5)$$

The hyperbolic embedding surface has two radii of curvature, R_1 and R_2 , approximated by the average radii of the 'inner' and 'outer' tunnels on either side of the surface. (If the embedding surface is a minimal surface, these radii are of equal magnitude.) Both tunnel systems are spanned by the 'inner' and 'outer'

collar rings, whose average ring sizes are denoted n_{col}^1 and n_{col}^2 . These ring sizes allow estimates of the two radii of curvature:

$$R_1/R_2 \approx n_{\text{col}}^1/n_{\text{col}}^2.$$

The separation between the embedding surface and the (parallel) minimal surface, x , can then be estimated, noting that $R_1 = (R - x)$ and $R_2 = (R + x)$, where the larger collar ring is n_{col}^2 . Expansion of R_1/R_2 to linear order gives

$$(x/R)^2 \approx [1 - (n_{\text{col}}^1/n_{\text{col}}^2)]^{1/2}]^2. \quad (6)$$

The homogeneity index for the embedding, H , is then related to that of the minimal surface, H_0 (assumed to be $3/4$), by combining (1), (5) and (6):

$$H = H_0\{1 - [1 - (n_{\text{col}}^1/n_{\text{col}}^2)]^{1/2}\}^{3/2}. \quad (7)$$

Equation (7) is an estimate, valid only for embedding surfaces of small mean curvature compared with the net edge length.

The net densities and the square roots of the integral curvatures of the graphs in their 'minimal embeddings' are plotted in Fig. 1.

According to (4), if the area Ω is independent of the curvatures of the embedding, the plot should be linear. Indeed, the graph exhibits a nearly linear trend over a range of curvatures. A least-squares linear fit of the data through the origin gives the approximate relation

$$\Omega = 1.3l^2. \quad (8)$$

The presence of deviations from this relation points to variations in the scaled area per vertex in three-dimensional periodic nets in their maximum-volume configurations. In order to arrive at a better estimate of the relation between net density and ring sizes, *a priori* estimates of the area per vertex, Ω , are required.

Upper and lower bounds for the area per vertex (Ω_{max} and Ω_{min}) can be obtained by comparing the area of the hyperbolic embedding surface in the vicinity of a vertex with its planar projection onto the hyperbolic plane and the Euclidean (flat) plane respectively.

As the Gaussian curvature becomes increasingly negative, the area of the embedding surface must increase. Consequently,

$$\Omega_{\text{min}} = (zl^2/4)\tan(\pi/z) \quad (9)$$

since the expression is equal to the area of the Voronoi region about each vertex (a z -gon of inradius $l/2$) in the planar embedding surface of a z -connected net (*i.e.* the area projected onto the Euclidean plane).

An upper bound for the area per vertex can be derived by noting that the embedding surface must have an area smaller than that of a surface of

Table 1. *List of three-, four-, five- and six-connected nets included in this analysis*

The embedding surface is listed (*italicised* if it is not minimal). Also included are the connectivity (z), the ring sizes on the surface, the average surface ring size (n_2), the size of the 'collar rings' (which surround tunnels and are not spanned by the surface), n_{col} , the homogeneity index (H), the scaled density (r) and r/H .

Net	Space group	Surface	z	Two-dimensional		n_2	n_{col}^1	n_{col}^2	H	r	r/H	Source of r
				rings								
ThSi ₂	<i>I4₁/amd</i>	CLP	3	12.12.12	12	$x\text{\S}$	x	0.75	0.44	0.59	(a)	
SrSi ₂	<i>I4₁32</i>	Gyroid	3	10.10.10	10	x	x	0.75	0.35	0.47	(b)	
8.8.8 ₂ †	<i>Im3m</i>	I-WP	3	8.8.8	8	x	x	0.75	0.34	0.46	(a)	
4.12 ₂ .12 ₂	<i>Im3m</i>	D	3	4.12.12	7.20	x	x	0.75	0.21	0.28	(a)	
Polybenzene	<i>Pn3m</i>	D	3	6.8.8	7.20	12	12	0.75	0.31	0.42	(b)	
6.8 ₂ /P	<i>Im3m</i>	P	3	6.8.8	7.20	12	12	0.75	0.33	0.44	(b)	
Hyperbolic graphite	<i>Fd3m</i>	D	3	6.8	6.26	x	x	0.75	0.15	0.20	(c)	
Hyperbolic graphite	<i>Im3m</i>	P	3	6.8	6.26	x	x	0.75	0.14	0.19	(c)	
Hyperbolic graphite	<i>Ia3d</i>	Gyroid	3	6.8	6.26	x	x	0.75	0.15	0.21	(c)	
Hyperbolic graphite	<i>I43m</i>	I-WP	3	5,6,8	6.20	x	x	0.75	0.15	0.19	(c)	
Schwarzite D	<i>Pn3</i>	D	3	6,7	6.23	x	2x	0.65	0.16	0.25	(d)	
Schwarzite P	<i>Ia3</i>	P	3	6,7	6.23	x	2x	0.65	0.14	0.22	(d)	
Schwarzite G	<i>Ia3d</i>	Gyroid	3	6,7	6.23	x	x	0.75	0.17	0.23	(e)	
Buckygym	<i>Fd3</i>	D	3	6,7	6.15	x	1.7x	0.75	0.07	0.10	(f)	
CdSO ₄	<i>P4₂/mmc</i>	<i>tD</i>	4	8.8.8.8	8	8	8	0.75	1.00	1.33	(g)	
NbO	<i>Im3m</i>	<i>D</i>	4	6.6.6.6	6	8	8	0.75	0.75	1.00	(a)	
S*	<i>Ia3d</i>	Gyroid	4	6.6.6.6	6	6	6	0.75	0.69	0.92	(a)	
Diamond	<i>Fd3m</i>	—	4	6.6.6.6	6	6	6	0.75	0.65	0.86	(a)	
Lonsdaleite	<i>P6₃/mmc</i>	—	4	6.6.6.6	6	6	6	0.75	0.65	0.86	(a)	
CrB ₄	<i>I/mmm</i>	<i>tP</i>	4	4.6.6.6	5.33	6	6	0.75	0.63	0.84	(a)	
CaGa ₂ O ₄	<i>Cmca</i>	<i>oDb</i>	4	4.6.6.6	5.33	6	6	0.75	0.62	0.82	(a)	
MEP†	<i>Pm3n</i>	—	4	—	5.08	6	6	0.75	0.58	0.77	(h)	
CAN	<i>P6₃/mmc</i>	<i>H</i>	4	4.4.6.6	4.80	6	6	0.75	0.53	0.71	(a)	
SOD	<i>Im3m</i>	<i>D</i>	4	4.4.6.6	4.80	6	6	0.75	0.53	0.71	(g)	
<i>SOD</i>	<i>Im3m</i>	<i>P</i>	4	6.6.6.6	6	4	4	0.75	0.53	0.71	(a)	
AST/octadecasil	<i>Fm3m</i>	<i>tP</i>	4	—	5	6	6	0.75	0.50	0.67	(a)	
GME	<i>P6₃/mmc</i>	<i>H</i>	4	4.4.4.8	4.57	6	8	0.73	0.45	0.62	(a)	
KFI	<i>Im3m</i>	I-WP	4	4.4.4.8	4.57	6	8	0.73	0.45	0.61	(a)	
LTA	<i>Pm3m</i>	<i>P</i>	4	4.4.6.6	4.80	4	8	0.66	0.43	0.65	(a)	
RHO	<i>Im3m</i>	<i>P</i>	4	4.4.4.6	4.36	8	8	0.75	0.43	0.57	(a)	
FAU	<i>Fd3m</i>	<i>D</i>	4	4.4.4.6	4.36	6	12	0.66	0.38	0.58	(a)	
<i>W*8</i>	<i>Im3m</i>	I-WP	4	4.4.4.8	4.57	4	12	0.56	0.30	0.54	(g)	
<i>W*4</i>	<i>Im3m</i>	<i>D</i>	4	3.8.3.12	4.57	3	12	0.49	0.20	0.40	(g)	
3.4 ⁴	<i>Pm3m</i>	<i>P</i>	5	3.3.3.3.4	3.75	4	8	0.66	0.60	0.92	(a)	
3 ³ .6 ²	<i>Fd3m</i>	<i>D</i>	5	3.3.3.6.6	3.75	6	12	0.66	0.44	0.67	(a)	
3.4 ⁴	<i>Fd3m</i>	<i>D</i>	5	3.4.4.4.4	3.75	6	6	0.75	0.71	0.95	(a)	
CaB ₆	<i>Pm3m</i>	I-WP	5	8.3.3.3.8	4.00	3	6	0.66	0.43	0.65	(a)	
P/D saddle polyhedral skeletal net	<i>Pn3m</i>	<i>D</i>	6	4.4.4.4.4.4	4	6	6	0.75	1.41	1.89	(i)	
P/D saddle polyhedral skeletal net	<i>Im3m</i>	<i>P</i>	6	6.6.6.6.6.6	6	4	4	0.75	1.41	1.89	(i)	

References: (a) O'Keeffe & Hyde (1994); (b) O'Keeffe, Adams & Sankey (1992); (c) Terrones & Mackay (1993); (d) Lenosky, Gonze, Teter & Elser (1992); (e) Mackay & Terrones (1993); (f) Vanderbilt & Tersoff (1991); (g) O'Keeffe (1991); (h) Hyde (1993); (i) Hyde & Andersson (1984).

† These numbers are the extended Schlaefli symbols of O'Keeffe.

‡ The three-letter codes denote zeolite nets, listed by Meier & Olson (1992).

§ x denotes the fact that actual tunnel ring sizes are unknown. The ratios of tunnel sizes are used instead.

constant Gaussian curvature (K_{H^2} , which is negative), *i.e.* a hyperbolic plane,* where the magnitude of the Gaussian curvature ($-K_{H^2}$) is at least as large as the maximum magnitude of the Gaussian curvature on the embedding surface. For the hyperbolic plane, the curved area (Ω) is related to its projected area (A) onto the Euclidean plane by the approximate expression (Robertson, 1990)

$$\Omega = A[1 - (K_{H^2}l^2/12) + \dots] \quad (10)$$

* In fact, the area of the hyperbolic plane is so large that it cannot be realised in \mathbb{R}^3 without singularities.

For smooth hyperbolic surfaces in \mathbb{R}^3 , the Gaussian curvature necessarily varies over the surface. For quasi-homogeneous triply periodic minimal surfaces, the maximum magnitude of the Gaussian curvature is typically 50% larger than the average value of the Gaussian curvature, $\langle K \rangle$, defined by

$$\langle K \rangle \equiv \frac{\int_{\text{unit cell}} K da}{\int_{\text{unit cell}} da}$$

This implies the approximate relation from (10):

$$\Omega \approx A[1 - (\langle K \rangle l^2/8)]. \quad (11)$$

(In fact, it turns out that the final estimate is rather

insensitive to the exact value of the denominator in this equation.)

In order to derive an upper bound for Ω , an upper bound for the projected area, A , is needed. The projected area per n_2 ring is clearly less than that of a planar n_2 polygon of edge length l , viz $(n_2 l^2/4) \cot(\pi/n_2)$, so that

$$A < (z l^2/4) \cot(\pi/n_2). \quad (12)$$

The inequality is due to the fact that average ring sizes are used to determine the average projected area, whereas the area function is nonlinear. Thus,

$$\Omega < (z l^2/4) \cot(\pi/n_2) [1 - (\langle K \rangle l^2/8)]. \quad (13)$$

Multiplying both sides by Ω , noting that $\langle K \rangle \Omega$ is fixed *via* the equation $\langle K \rangle \Omega = \int K da = 2\pi\chi$ and is therefore known, and solving for Ω gives an estimate of the upper bound:

$$\Omega_{\max} = (A/2) \{1 + [1 - (\langle K \rangle \Omega l^2/2A^2)]^{1/2}\}, \quad (14)$$

where A is given by (12) and $\langle K \rangle \Omega = 2\pi[z + (1 - z/2)n_2]/n_2$.

These expressions for Ω_{\min} and Ω_{\max} admit estimates of the range of accessible net densities as a function of the average surface ring size, n_2 , and the connectivity of the net, z , using (4), (9) and (14). The net data displayed in Table 1 (including embeddings that are not minimal) are plotted in Figs. 2(a), (b), (c) and (d) below, together with the plots of the maximum and minimum estimated densities [using Ω_{\min} and Ω_{\max} in (4), respectively].

Validity of the analysis

The equations above offer appropriate bounds on the density for most nets considered here. Provided

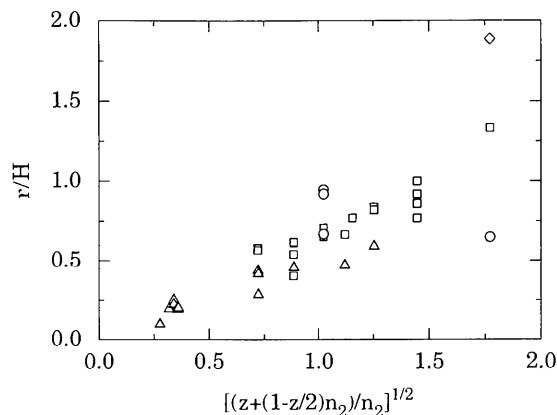


Fig. 1. Plot of scaled net density, r , divided by the homogeneity index, H , as a function of average curvature, $\{2\pi[z/n_2 + (1 - z/2)]\}^{1/2}$ (z and n_2 denote the net connectivity per vertex and average surface ring size, respectively), for 'minimal embeddings'. Triangles denote three-connected nets, squares four-connected nets, circles five-connected nets and diamonds six-connected nets.

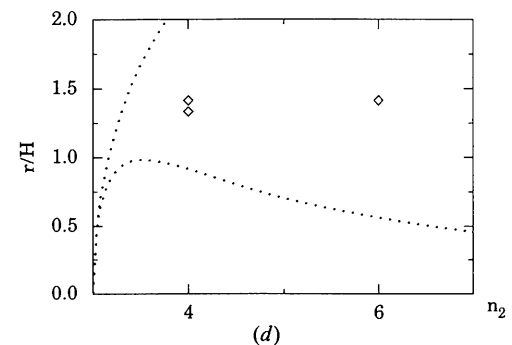
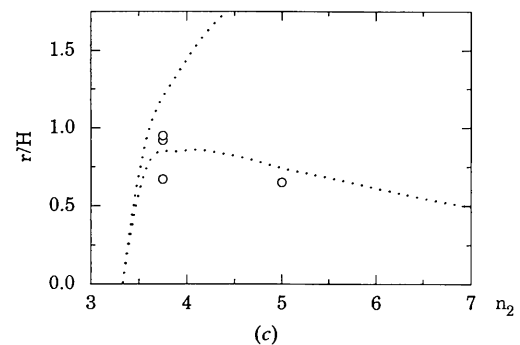
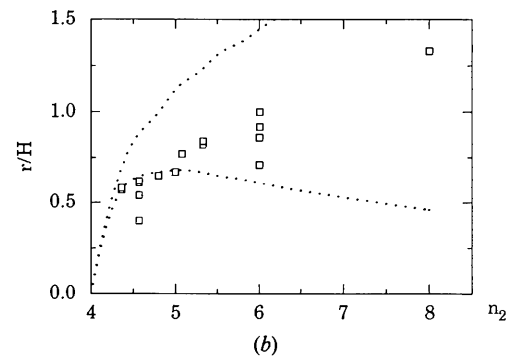
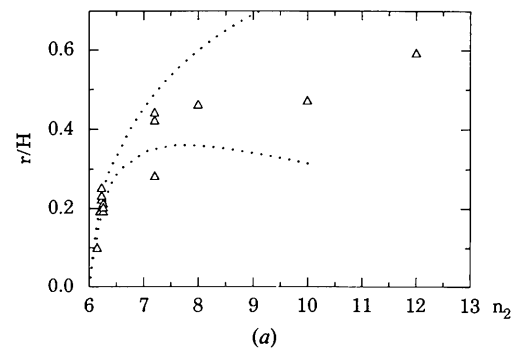


Fig. 2. (a) Plot of net density (r)/homogeneity index (H) versus average ring size in the embedding surface (n_2) for a range of three-connected nets of equal edge length (Table 1). The dotted curves are plotted using (4) and (9) (upper curve) and (4) and (14) (lower curve). These curves define upper and lower bounds on the net density for 'quasi-uniform' nets (approximately equal vertex angles and surface ring sizes). (b) Plot as in (a) for four-connected nets. (c) Plot as in (a) for some five-connected nets. (d) Plot as in (a) for some six-connected nets.

the variation of surface ring sizes in the net is small and the net lies on a quasi-homogeneous embedding surface, the nets lie within the expected density limits.

However, the lower bound for the density fails to account for some rare three- and four-connected nets discussed by O'Keeffe, namely the Y^*3 and 4.12^2 three-connected nets (O'Keeffe & Hyde, 1994), and the W^*8 and W^*4 four-connected nets (O'Keeffe, 1991). These violations can be traced to the averaging procedure used to derive the equations for the most dense and rarest nets. A single measure of the net topology has been used; the average ring size of those rings lying in the surface.† The averaging underestimates the projected area per vertex, A , used to derive Ω_{\max} above. Significant deviations from the flat area per vertex expected from (12) occur when some surface rings are small and others are large, *i.e.* as in the Y^*3 , 4.12^2 , W^*8 and W^*4 nets. Calculations show that this effect can double the area A (*e.g.* 4- and 12-rings in a three-connected net) and the minimum density can be lower than that predicted here by a factor of three. In fact, this suggests a useful route to constructing rare nets, *viz* fusing small and large rings, already exploited by O'Keeffe. This effect is expected to be significant only for intermediate values of n_2 , since low n_2 values cannot be sustained simultaneously with very different surface ring sizes, and high values lead to approximately linear behaviour in (12). Recall, also, that these bounds have been derived for quasi-uniform nets, *viz* equal edge lengths, vertex angles and torsion and ring sizes.

The presence of a maximum in the curves defining the relations between minimum density and ring size (Fig. 2) is related to the possibility of embeddings other than the minimal embedding, discussed above. In general, at least two embeddings are possible (corresponding to 'complementary' surfaces, sharing the same network (Hyde & Andersson, 1984). Indeed, it is possible to construct embeddings for which all the rings in the net defined collar rings, in which case n_2 diverges (and $\chi/N = -1$). The large n_2 limit of the lower curves in Fig. 2 must thus be vanishingly small. At the other extreme of Gaussian curvature ($\chi/N = 0$), the density must scale similarly to that of a planar net (*i.e.* increase with n_2). These asymptotic forms imply the presence of at least a single maximum in the curve, as found. The location of the maximum is around average ring sizes of five. I suggest that the region of rare nets on the right-hand branch of this curve (*i.e.* $n_2 > 5$) represents

non-minimal embeddings, whose minimal embeddings occur on the left-hand branch.

The density of tectosilicates

The trend of increasing density with surface ring size observed in minimal embeddings of silicon-rich zeolite frameworks (Hyde *et al.*, 1993) is also followed by the nets considered here (Fig. 1). However, this relation is violated in some cases, as expected from the analysis plotted in Fig. 2, which shows that a range of densities are geometrically accessible when the average ring size of the framework becomes large (*e.g.* >5 for four-connected frameworks). But the analysis above is strictly geometric in nature and extra constraints beyond those imposed by Euclidean three-dimensional space may be at work in chemical, frameworks. Framework densities of some silicates,

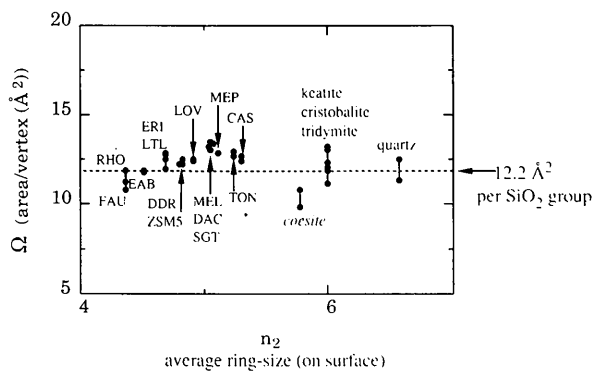


Fig. 3. Plot of the curved surface area per TO_2 group for a range of silicon-rich zeolites (Si:Al ratio >3) and the area per SiO_2 group for clathrasils and dense silicates. The three-letter codes are those listed by Meier & Olson (1992). Upper and lower bounds for the area are plotted for frameworks with more than a single type of vertex. The average of these data, 12.2 \AA^2 per vertex, is indicated by the dotted line.

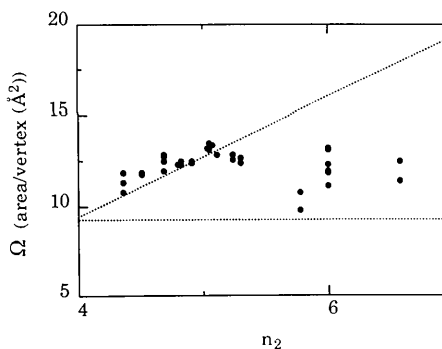


Fig. 4. Plot of the data in Fig. 3, together with upper and lower bounds on the areas per vertex set by geometry alone.

† This average is a weighted one, since large rings 'see' more vertices than small rings. For example, a four-connected net, with rings (a, b, c, d) on the surface, gives a ring size of $n_2 = 4/(a^{-1} + b^{-1} + c^{-1} + d^{-1})$.

silicides, germanides and water frameworks suggest that the area per vertex, Ω , varies little as a function of the framework curvature, for a fixed framework composition (Hyde, 1993).

From O'Keeffe's (1991) network classification, the average surface ring size for the minimal embedding of any network containing equivalent vertices (or, alternatively, the characteristic of the network, γ) can be readily determined (Hyde, 1993). The area per vertex, Ω , can then be deduced from (4) and (7). Where more than one type of vertex is present in a net, upper and lower bounds on the average surface ring size can be found. Fig. 3 shows the area, Ω , of a range of silicon-rich zeolites, clathrasils and dense silicates, using standard data for the framework density, assuming a distance of 3.05 Å between the T-atom vertices. With the exception of the densest four-connected silicate framework, coesite, the frameworks exhibit approximately equal area per vertex, regardless of the curvature of the framework.

These data are plotted with the maximum and minimum areas found according to (9) and (14) in Fig. 4. Geometrical considerations alone allow the areas to vary between these limits, under the assumption of quasi-uniform networks. Clearly, the weak variation of surface areas with silica-framework curvature is not due to the geometry of Euclidean three-dimensional space. Rather, this effect must be set by interatomic interactions at work within these covalent frameworks.

I thank Professor Michael O'Keeffe for many stimulating discussions.

Acta Cryst. (1994). **A50**, 759–771

On the Validity of the Direct Phasing and Fourier Method in Electron Crystallography

BY L.-M. PENG AND S. Q. WANG*

Department of Materials, University of Oxford, Parks Road, Oxford OX1 3PH, England

(Received 31 January 1994; accepted 25 May 1994)

Abstract

The validity of the direct phasing and Fourier method for direct crystal structure determination is examined. It is shown that, while the kinematic approximation for electron diffraction is not strictly valid for all materials containing heavy atoms in real

* Also at Beijing Laboratory of Electron Microscopy, Chinese Academy of Sciences, Beijing, People's Republic of China.

References

- ANDERSSON, S., HYDE, S. T., LARSSON, K. & LIDIN, S. (1988). *Chem. Rev.* **88**, 221–242.
- BRUNNER, G. O. & MEIER, W. M. (1989). *Nature (London)*, **337**, 146–147.
- COXETER, H. S. M. (1937). *Proc. London Math. Soc. Second Ser.* **43**, 33–62.
- FIRBY, P. A. & GARDINER, C. F. (1991). *Surface Topology*. Chichester: Ellis Horwood Ltd.
- HYDE, S. T. (1992). *Pure Appl. Chem.* **64**(11), 1617–1622.
- HYDE, S. T. (1993). *Defects and Processes in the Solid State. Some Examples in Earth Sciences*, edited by J. BOLAND & J. FITZGERALD, pp. 317–342. Amsterdam: Elsevier.
- HYDE, S. T. & ANDERSSON, S. (1984). *Z. Kristallogr.* **168**, 221–254.
- HYDE, S. T., BLUM, Z. & NINHAM, B. W. (1993). *Acta Cryst.* **A49**, 586–589.
- LENOSKY, T., GONZE, X., TETER, M. & ELSER, V. (1992). *Nature (London)*, **355**, 333–335.
- LINDSAY, J. H. (1959). *Am. Math. Mon.* **36**, 117–118.
- MACKAY, A. L. & TERRONES, H. (1993). *Philos. Trans. R. Soc. London (Phys. Eng.)*, **343**, 113–127.
- MEIER, W. M. (1986). *Pure Appl. Chem.* **58**, 1323–1328.
- MEIER, W. M. & OLSON, D. H. (1992). *Atlas of Zeolite Structure Types*. London: Butterworth-Heinemann.
- O'KEEFFE, M. (1991). *Z. Kristallogr.* **196**, 21–37.
- O'KEEFFE, M., ADAMS, G. B. & SANKEY, O. F. (1992). *Phys. Rev. Lett.* **68**(15), 2325–2328.
- O'KEEFFE, M. & HYDE, B. G. (1994). Book to be published by World Scientific Press, Singapore.
- ROBERTSON, H. P. (1990). *The Encyclopedia of Physics*, p. 266. New York: Simon and Schuster.
- SMITH, J. V. (1988). *Chem. Rev.* **88**, 149–182.
- STIXRUDE, L. & BUKOWINSKI, M. S. T. (1990). *Am. Mineral.* **75**, 1159–1169.
- TERRONES, H. & MACKAY, A. L. (1993). *Chem. Phys. Lett.* **207**(1), 45–50.
- VANDERBILT, D. & TERSOFF, J. (1991). *Phys. Rev. Lett.* **68**, 511–513.
- WELLS, A. F. (1977). *Three-Dimensional Nets and Polyhedra*, p. 160. New York: Wiley.

space, many of the low-order diffracted beams behave kinematically for a small crystal thickness. For thin crystals, structure maps constructed from compound crystals containing heavy atoms using low-order reflections are found to be faithful representations of the crystal structures. The inclusion of high-order diffracted beams is shown, however, to introduce intensity maxima that do not coincide with atom positions. It is shown that, if dynamical phases